

Laser-induced coherent acoustical phonons mechanisms in the metal-insulator transition compound NdNiO₃: Thermal and nonthermal processes

P. Ruello,^{1,*} S. Zhang,² P. Laffez,¹ B. Perrin,² and V. Gusev¹

¹Laboratoire de Physique de l'État Condensé, UMR CNRS 6087, Université du Maine, 72085 Le Mans, France

²Institut des NanoSciences de Paris, UMR CNRS 7588, rue Lourmel, 75015 Paris, France

(Received 16 September 2008; revised manuscript received 24 January 2009; published 19 March 2009)

Coherent acoustic phonon generation processes on the picosecond time scale were investigated in the metal-insulator transition compound NdNiO₃. Time-resolved optical pump-probe methods were employed. While at high temperature thermoelastic process drives the photogeneration of acoustic phonons, an additional contribution can be identified when the transition to the insulating state at $T < T_{MI}$ takes place. The latter additional photogenerated stress is possibly of electronic stress nature (deformation-potential mechanism). We show that it competes with thermoelastic stress, leading to reduction in the magnitude of a photogenerated acoustic phonon pulse. In that insulating state, we suggest that the electron-phonon deformation-potential coupling in NdNiO₃ leads to a laser-induced lattice cell volume contraction. Furthermore, in the temperature range where a first-order phase transition takes place and where both metallic and insulating metastable phases coexist, the photogenerated ultrashort picosecond acoustic pulse magnitude cannot be described by a classical thermoelastic process. We suggest that such a phenomenon is connected to unusual thermoelasticity in a metastable state. In particular, we discuss the definition of the thermal-expansion coefficient of solids in a metastable state subjected to ultrafast optical excitation.

DOI: [10.1103/PhysRevB.79.094303](https://doi.org/10.1103/PhysRevB.79.094303)

PACS number(s): 71.30.+h, 63.20.kd, 78.47.-p

I. INTRODUCTION

Femtosecond laser-based acoustics has opened the field of time-resolved investigations of complex electron-lattice interactions through the study of sound photogeneration mechanisms.¹⁻⁵ When dealing with acoustic phonon photogeneration processes in opaque materials,^{2,3} two mechanisms are commonly involved. The first process (nonthermal) is based on a deformation-potential mechanism and exists as soon as electrons undergo a spatial redistribution after pump quanta excitation. This redistribution of photoexcited electrons induces a perturbation of the internal electric field which consequently forces cations to displace from their original place. It can also be viewed as a pump light-induced change in the population of electrons in the bands (orbitals). Consequently, this change in electronic distribution modifies the local overlapping of orbitals which consequently modifies the position of nucleus. Compressive or tensile stress can then be obtained depending on the sign of the electron-acoustic phonon deformation-potential coefficient.⁶⁻⁸ This nonthermal process starts immediately after pump quanta absorption occurs and lasts as long as the electronic cloud is out of equilibrium.^{2,3} After the pump excitation, and when the electron-electron thermalization is achieved after a typical time of 100 fs, the electronic subsystem starts to transfer its energy to the phononic subsystem. That transfer occurs by phonon emission. It is the second process, usually called a thermoelastic process. This process is driven by the electron-phonon thermalization whose characteristic relaxation time is typically around 1 ps, and occurs in the metals as well as in conduction and valence bands of semiconducting materials.⁹⁻¹¹ During that thermal process, a rapid local increase in phonon emission produces a rapid heating of the lattice. Because of anharmonicity of the lattice, this increase in temperature produces a thermoelastic stress giving rise to

an acoustic wave generation.² These nonthermal and thermal contributions lead to the general expression of the stress tensor:²

$$\sigma_{ij} = \sum_{\vec{k}} \Delta n_e(\vec{k}) \frac{\partial E_{\vec{k}}}{\partial \eta_{ij}} + \sum_{\vec{q}} \Delta n_p(\vec{q}) \hbar \frac{\partial \omega_{\vec{q}}}{\partial \eta_{ij}} = \sigma_e + \sigma_p, \quad (1)$$

where η_{ij} , $\Delta n_e(\vec{k})$, $\Delta n_p(\vec{q})$, $\frac{\partial E_{\vec{k}}}{\partial \eta_{ij}}$, and $\frac{\partial \omega_{\vec{q}}}{\partial \eta_{ij}}$ are the strain tensor, the modification of the electronic population in the level $E_{\vec{k}}$, the modification of the phonon population in the level $\hbar \omega_{\vec{q}}$, the deformation-potential parameter associated with the electronic level $E_{\vec{k}}$, and the volume dependence of the phonon frequency $\omega_{\vec{q}}$. The first term in Eq. (1) corresponds to the electronic stress and the second one corresponds to the phononic stress (thermoelastic stress). The latter stress is connected to Grüneisen coefficient $\gamma_{\vec{q}} = -\frac{\partial \ln(\omega_{\vec{q}})}{\partial \ln(V)}$ associated with the mode $\omega_{\vec{q}}$. If we consider the Grüneisen coefficient γ_L characterizing the integrated anharmonicity of the entire modes of the crystal,¹² the thermoelastic stress in an isotropic medium reduces to $\sigma_p = -\sum_{\vec{q}} \Delta n_p(\vec{q}) \hbar \omega_{\vec{q}} \gamma_{\vec{q}} = -\gamma_L C_L \Delta T_L$, where C_L and ΔT_L are the heat capacity and photoinduced lattice temperature increase. The thermoelastic stress can also be written as $\sigma_p = -3B\beta \Delta T_L$ since $\beta = \frac{\gamma_L C_L}{3B}$,¹² where B and β are the bulk modulus and the thermal-expansion coefficient.

Whatever thermal or nonthermal processes are involved, the photoinduced stress is spatially inhomogeneous due to the existence of surfaces (semi-infinite system) or interfaces (layered system). Such inhomogeneities are also usually due to an exponential shape of the depth profile of the pump radiation absorption in an opaque system. So as soon as a gradient of each of these stresses exists, a force appears, provoking atoms to be accelerated, giving rise to an acoustic

wave. The particle acceleration in an isotropic medium is described as follows:³

$$\rho_0 \frac{\partial^2 u(t,z)}{\partial t^2} = \frac{\partial \sigma(t,z)}{\partial z} = \rho_0 v^2 \frac{\partial^2 u(t,z)}{\partial z^2} + \frac{\partial(\sigma_e + \sigma_p)}{\partial z}, \quad (2)$$

where ρ_0 , u , and v are the density, the acoustic displacement, and the longitudinal speed of sound. Sound propagation is normal to the irradiated surface and occurs in the $+z$ and $-z$ directions. Therefore, by analyzing the time and temperature dependence of the laser-induced acoustic pulse, it is then possible to extract the physical parameters of the initial electron–acoustic phonon coupling.

It is well known that compounds exhibiting phase transitions present large temperature variations of the electron-phonon and the phonon-phonon coupling, which makes them particularly good candidates for studying the contribution of the different mechanisms of ultrafast acoustic phonon generation. Coherent acoustic phonon generation has already been investigated in the manganite compound $\text{La}_{1-x}\text{Ca}_x\text{MnO}_3$, where thermoelasticity was claimed to be the driving mechanism.¹³ Recent investigations on ferromagnetic superlattices with ultrafast x-ray diffraction have also revealed interesting competing behaviors between phonon-mediated stress (thermoelastic stress) and magnetostrictive stress.^{14,15} In our studies we have chosen a metal-insulator transition (MIT) compound which exhibits two interesting properties. First of all, the transition is first-order-like^{16–21} with a drastic temperature change of lattice thermal expansion which can potentially modulate the magnitude of the thermoelastic coupling as a function of temperature. Second, the electronic band structure exhibits large variation when a pseudogap opens in the insulating state ($T < T_{\text{MI}}$).^{22–25} That temperature variation of the electronic band structure is then favorable for potentially modulating the contribution of the deformation-potential electron–acoustic phonon coupling. That last point has been the subject of several studies in RNiO_3 compounds since extraordinary pressure dependence of crystallographic structure²⁶ as well as electrical transport^{27,28} suggests that a particular electron–acoustic phonon coupling should take place.

In a previous study²⁹ we have shown some peculiar temperature dependence of acoustic waves generated by femtosecond laser pulses but no systematic temperature studies were performed, preventing a clear understanding of its origin. In this paper, we present a comprehensive study of the temperature dependence of the electron-lattice coupling through a phase transition by picosecond acoustics. Moreover, in addition to the reflectometric setup which allows detection of acoustic strain, we have employed in this study an interferometric setup. Such a setup is well known to provide more information on the acoustic pulse since it probes both the acoustic strain and the acoustic displacement.³⁰

II. EXPERIMENTAL RESULTS

A. Sample preparation and experimental setup

The same film of NdNiO_3 of 150 nm thickness, deposited on (100) silicon substrate, as employed in previous stud-

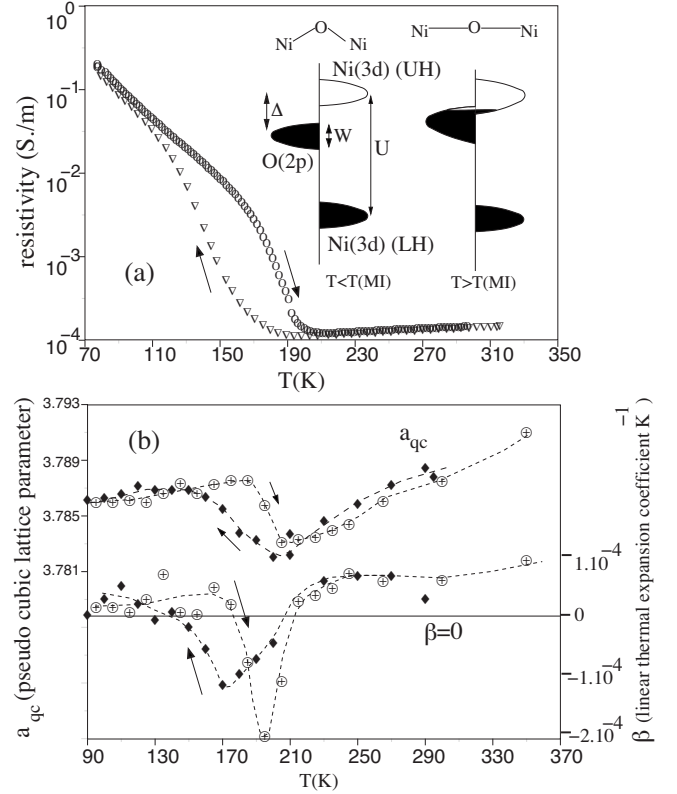


FIG. 1. (a) Four-wire dc electrical conductivity versus temperature (taken from Ref. 32). The inset is a sketch of the valence-band picture where Δ , U , UH and LU , and W are the charge-transfer gap, the Hubbard gap, the upper and lower Hubbard bands, and the O_{2p} -like band width. At T_{MI} the gap closes. (b) Pseudocubic out-of-plane lattice parameter versus temperature and the associated thermal-expansion coefficient calculated by smoothed finite differences.

ies^{29,31,32} was used. The NdNiO_3 material was grown by radio-frequency reactive magnetron sputtering performed at 873 K. The target was a mixture of polycrystalline NiO and Nd_2NiO_4 . A postannealing at 1073 K under high oxygen pressure (180 bar) was then achieved. During annealing, a thin silica layer (~ 10 nm) is formed between film and silicon substrate. The temperature of the MIT found in four-wire dc electrical conductivity measurements is close to 190 K (heating regime) and 160 K (cooling regime)^{29,32} [see Fig. 1(a)] as expected for a bulk sample.^{18,33} The temperature variation of the out-of-plane pseudocubic cell parameter is reported in Fig. 1(b) with the thermal-expansion coefficient determined by smoothed finite differences. Its temperature behavior is consistent with literature.^{17,19,21} The abrupt change in the lattice parameter and hysteresis loop clearly shows the first-order nature of the transition, in agreement with literature.^{16,18} For the time-resolved optical properties measurements, a Sagnac interferometer pump-probe setup was used with a Ti:sapphire oscillator of 120 fs pulse width working at a repetition rate of 81 MHz.^{30,34} For the transient reflectometric measurements a cross-polarized pump-probe experiment was achieved with a Ti:sapphire oscillator of 120 fs pulse width. The sample was placed in either a helium-cooled or nitrogen-cooled cryostat.²⁹ In both experiments,

the reflection geometry was chosen. In order to detect small pump-induced changes in the sample reflectance, the pump beam was modulated at either 800 kHz or 1 MHz with an acousto-optic modulator (AOM). The probe signals were then collected by a photodiode and processed with a lock-in amplifier. It is worth mentioning that reflectometric and interferometric measurements are complementary in laser ultrasonics since we have access either to the real (ρ reflectometry) or the imaginary ($\delta\phi$ interferometry) part of the optical complex reflectivity coefficient. The general formulation of the transient complex reflectance is^{30,35}

$$\begin{aligned} dr/r &\approx \rho + i\delta\phi \\ &\approx -2ik_0\delta z + \frac{4ik_0n}{(1-n^2)} \frac{dn}{d\eta} \int_0^\infty \eta(z,t) \exp(2ik_0nz) dz, \end{aligned} \quad (3)$$

where $n=n'+in''$ is the refractive index at the probe wavelength, $k_0=2\pi/\lambda$ is the probe wave vector in air, $\eta(z,t)$ is the acoustic strain propagating perpendicularly to the surface of the sample, and $dn/d\eta$ is the photoelastic coefficient. $z=0$ corresponds to the interface air/material. In the expression of the complex optical reflectivity, the first term corresponds to the contribution of the surface displacement (δz) and the second one corresponds to the photoelastic contribution.

In our experiments, the probe and pump wavelengths were both 760 nm. At the wavelength of $\lambda=760$ nm the typical optical-absorption length was estimated to be ~ 60 nm for NdNiO₃.²² The probe and pump are both focused on the sample with a lens leading to a pump and probe spot diameter of ~ 50 μm . The energy density was ~ 100 $\mu\text{J cm}^{-2}$, which gives a photoexcited electron concentration of around 10^{19} cm^{-3} , which corresponds to around one photoexcited electron per one thousand NdNiO₃ unit cells. It has been checked that such pump fluence belonged to a linear-response regime of the material. Since the repetition rate of the laser pulses is high, some static heating takes place in the sample, which we estimate to be around 8 K.

B. Results and discussion

The transient optical signal is composed of a sharp electronic contribution followed by periodically separated acoustic echoes for both interferometric and reflectometric measurements as shown in Figs. 2(a) and 2(b). After the photogeneration of the acoustic phonon pulse on the free surface of NdNiO₃, the phonons propagate indeed through the entire film and undergo successively several acoustic reflections at the film/substrate and air/film interfaces. A ratio of 0.4 in magnitude between successive echoes is in agreement with our estimate. Details of acoustic echoes are given in the inset of both experiments [Figs. 2(a) and 2(b)]. While the echoes are detectable over the whole temperature range of investigation in phase signal ($\delta\phi$), they are undetectable in the amplitude signal (ρ) below around 124 K.

No appreciable modification of the shape of the acoustic pulse occurs through the phase transition [Fig. 3(a)]. On the other hand, an appreciable change in acoustic pulse magnitude happens for the $\delta\phi$ signal [Fig. 3(b)] with a decrease by

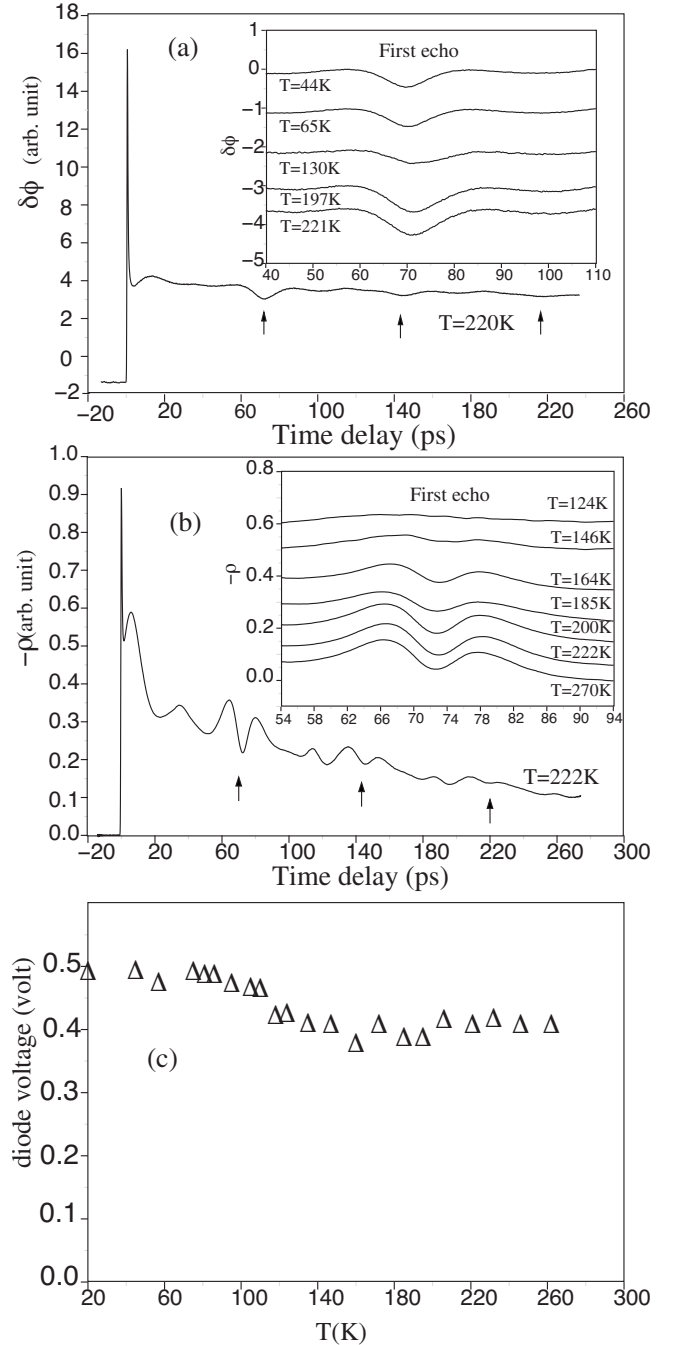


FIG. 2. (a) Transient optical interferometric signal at $T=220$ K. Inset: temperature variation in the first acoustic echo (the baseline was removed and the traces are displaced vertically for clarity). (b) Transient optical reflectometric signal at $T=222$ K. Inset: temperature variation of the first echo (the baseline was removed and the traces are displaced vertically for clarity). (c) Temperature dependence of the static reflectance of our sample at 760 nm given by the measured voltage on the photodetector (pin diode). In (a) and (b), the arrows indicate the first, second, and third detected acoustic echoes.

a factor of around 2 at low temperatures compared to the high-temperature regime. The decrease in the echo magnitude in the interferometric measurement is not perfectly monotonous and presents a minimum in the region of the tran-

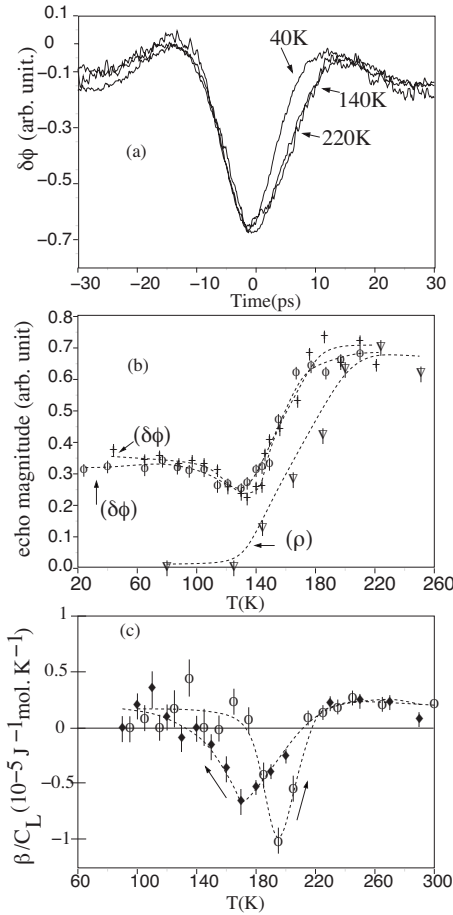


FIG. 3. (a) Comparison between normalized acoustic pulses detected in phase measurements ($\delta\phi$) for different temperatures. (b) Temperature dependence of the amplitude of first acoustic echo from interferometric [$\delta\phi$, heating (crosses) and cooling (circles) regimes] and reflectometric (ρ) measurements. (c) Temperature dependence of the ratio between linear thermal expansion and heat capacity (the heat capacity C_L was taken from Ref. 20). The β/C_L term determines the expected thermoelastic contribution to the coherent acoustic phonon generation.

sition as shown in Fig. 3(b). No similitude can be established with the temperature dependence of the echo magnitude (ρ signal), which rather exhibits a monotonous vanishing magnitude with decreasing temperature.

It is to be mentioned that such temperature dependence of the echo magnitude cannot be attributed to a temperature variation of the acoustic transmission coefficient due to the temperature evolution of the acoustic impedance of the film and that of the substrate. A rough estimation leads to a contribution below 1%.

The decrease in the acoustic pulse magnitude cannot be attributed to a variation in the optical properties of the NdNiO₃ compound. If a decrease by a factor of 2 of the magnitude of the photoexcitation of NdNiO₃ would occur, for example, below the transition temperature, this would require that the material optical-absorption depth should increase by a factor of around 2, which is not the case according to our following analysis. First, only a moderate variation [$<20\%$; see Fig. 2(c)] of the measured optical reflectivity

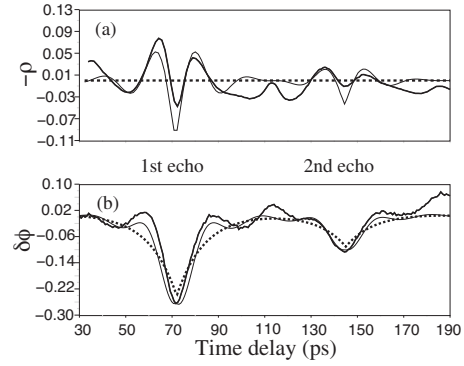


FIG. 4. Simulation of the first and second acoustic echoes detected in the reflectometric (ρ) and interferometric ($\delta\phi$) configurations. For both simulated signals (top and bottom), the thick solid line is the experimental measurement ($T=220$ K). The thin line is the best adjustment [$n \approx 2.7 + 0.8i$, $\partial n/\partial \eta \approx -0.1 - 2i$, and $V_{\text{NdNiO}_3} = 6200 \text{ m s}^{-1}$ (Ref. 36)]. The dashed lines are the simulated signals when the photoelastic coefficient vanishes ($\partial n/\partial \eta = 0$).

occurs at the probe wavelength, in agreement with literature.²² Second, following Eq. (3), we have adjusted the $\delta\phi$ signal as a function of temperature [see Fig. 4 (Ref. 36)]. Not only the complex refractive index n but also the photoelastic coefficient $\partial n/\partial \eta$ do not vary much within the range of our adjustment accuracy. Only the acoustic pulse magnitude changes significantly as a function of temperature [Fig. 3(b)]. It is indeed evident in Figs. 2(a) and 3(a) that the shape of the acoustic pulse is nearly constant over the whole temperature range. No broadening is seen as well. It is important to underline that the absence of the detection of the acoustic pulse in the ρ signal at low temperatures does not seem to be connected to the vanishing of the photoelastic coefficients. This can be checked by performing calculations (Fig. 4). If we consider indeed that the photoelastic coefficient $\partial n/\partial \eta$ becomes negligible, the acoustic pulse amplitude (ρ) would not only vanish [dashed line in Fig. 4(a)] but the shape of the acoustic pulse magnitude obtained in phase measurements ($\delta\phi$) would also change drastically [Fig. 4(b)] and should exhibit rather an exponential shape, like already observed for gold.³⁵ It is absolutely not the case for NdNiO₃. When photoelastic coefficients are negligible the shape of the acoustic echo in interferometric measurement is indeed simply exponential because it depends only on the surface displacement [$u(z=0, t) \approx e^{-\alpha v|t|}$].^{30,35} As a consequence, the vanishing of the photoelastic coefficients magnitude is unlikely. The origin of that strong decrease in the signal in amplitude (ρ) at low temperature is not easy to attribute, yet the origin of this phenomenon cannot be driven by temperature dependence of the photoelastic coefficients. For that reason, in the following we will concentrate the discussion on the imaginary part of the signal ($\delta\phi$).

Since the anomalous temperature dependence of the echo magnitude is not due to detection process, it appears that the observed effect must be connected to a special temperature dependence of the process of conversion of the energy from the photoexcited electron subsystem towards the lattice of the NdNiO₃ compound. As mentioned in Sec. I, one of the processes of acoustic wave generation is due to anharmonic

properties of the compound (thermoelastic coupling). As a first approximation, the magnitude of the acoustical strain driven by thermoelastic processes can be evaluated as² $\eta_0 = [(1-R)Q\beta]/(A\xi C_L)$, where R , Q , β , A , ξ , and C_L are the optical reflectivity coefficient, the optical energy of the pump beam, the thermal-expansion coefficient, the pump-irradiated surface, the optical penetration depth of the pump radiation, and the heat capacity. That strain magnitude is related to the laser-induced lattice temperature increase ΔT_L as $\Delta T_L = [(1-R)Q]/(A\xi C_L)$. In accordance with our previous discussion, it is admitted that the optical penetration depth of pump radiation (ξ) exhibits only slight variations (maximum of 20%), in agreement with literature.²² In the case of a pure thermoelastic contribution the driving parameter would then be the ratio between the thermal-expansion coefficient and the heat capacity.²⁰ Both these physical parameters exhibit a large temperature dependence. The temperature dependence of β/C_L is given in Fig. 3(c). When comparing Figs. 3(b) and 3(c), it is very interesting to note that their temperature dependences are drastically different. This phenomenon is different from that observed for the second-order phase transition compound $\text{La}_{1-x}\text{Ca}_x\text{MnO}_3$, where a rather good correspondence was found between the thermal expansion and the coherent acoustic phonon magnitude.¹³ Two points are remarkable in our experimental results:

(i) Well below the transition temperature the magnitude of the measured acoustic pulse does not follow that expected for the pure thermoelastic contribution where a comparable contribution should appear above and below the phase transition [Fig. 3(c)]. The ratio β/C_L is indeed of the same order of magnitude above ($T \gg T_{\text{MI}}$) and below ($T \ll T_{\text{MI}}$) the critical temperature.

(ii) It clearly appears that the measured acoustic pulse magnitude does not change its sign in the range of the temperature transition like the thermal-expansion coefficient does [Fig. 1(a)]. This observation suggests that the classical macroscopical thermal process does not drive the acoustic wave generation process.

In the following we analyze these two important points:

(i) It is known that the insulating state takes place below T_{MI} with a small pseudogap opening mechanism. Like in semiconductors, the existence of a gap can prevent photoexcited carriers to relax rapidly as discussed in a previous work.³² The out-of-equilibrium carriers provide a favorable situation for contribution of a stress of deformation-potential nature. In order to explain the decrease in the acoustic pulse magnitude at low temperatures, we can consider that a competition exists between the thermoelastic and the deformation-potential mechanisms. For that, σ_e and σ_p [see Eq. (1)] must be of the same order of magnitude but of opposite signs. As a consequence, the positive photoinduced electronic stress σ_e implies that among all electronic levels $E_{\vec{k}}$, the positive deformation-potential parameters $\frac{\partial E_{\vec{k}}}{\partial \eta_{ij}}$ are predominant. This means that when the lattice is compressed, the energy level $E_{\vec{k}}$ shifts toward a lower value. This also could be viewed as a lattice volume contraction when the electrons are promoted toward $E_{\vec{k}}$. In our case, since the pump quanta energy (1.6 eV) is close to the charge-transfer gap $\Delta \sim 1$ eV (Ref. 37) of NdNiO_3 , we suggest that the laser

excitation modifies the distribution of the effective charges located on Ni sites. This modification takes place over a typical time scale of the lifetime of the photoexcited carriers, ~ 2 ps.³² This means that the charge disproportionation would be optically reduced and probably partially melted. We recall that the MIT is proposed to be triggered by localization of charges on the Ni sites according to $2\text{Ni}^{3+} \rightarrow 2\text{Ni}^{(3+\delta)+} + \text{Ni}^{(3-\delta)+}$.^{38,39} In the case of a reduction in charge localization, we can easily understand that the lattice is forced to relax since it is well known that a strong coupling between localized charge carriers and the lattice distortion (polaron) takes place.^{40,41} Since that charge localization is accompanied by a volume increase,⁴² the light-induced reduction in charge localization will then lead to a volume contraction, consistent with our analysis of the competition between expansive thermoelastic and compressive electronic stresses. We have indications that our analysis appears to be relevant and that the deformation-potential parameter $\frac{\partial E_{\vec{k}}}{\partial \eta}$ is positive (or $\frac{\partial E_{\vec{k}}}{\partial P} = -B \frac{\partial E_{\vec{k}}}{\partial \eta}$ is negative). Several studies of the dependence of the transition temperature as a function of pressure have been carried out.²⁶⁻²⁸ It has been shown that the transition temperature detected through the analysis of the electrical conductivity decreases when isostatic pressure is applied²⁷ with $dT_{\text{MI}}/dP = -4.2$ K/kbar.²⁷ This result was considered as evidence of the closing of the pseudogap $E_g \approx \Delta - W$ of the insulating phase under pressure. This strongly supports then that $\frac{\partial E_g}{\partial P}$ is negative or $\frac{\partial E_g}{\partial \eta}$ is positive. The question now is the determination of the absolute value of the deformation-potential parameter. We can obtain first an estimate thanks to the following analysis of pressure dependence of the MIT. Considering indeed the rough scaling law $E_g \approx k_B T_{\text{MI}}$, and knowing that $dT_{\text{MI}}/dP = -4.2$ K/kbar,²⁷ we obtain then for the case of the insulating phase ($T < T_{\text{MI}}$) an estimate of the deformation-potential parameter of $dE_g/dP \approx k_B(dT_{\text{MI}}/dP) = -3 \times 10^{-12}$ eV Pa⁻¹. The deformation-potential coefficient can also be estimated according to a crystallographic investigation performed under pressure at different temperatures in PrNiO_3 .²⁶ In the following we assume the law deduced for PrNiO_3 to be valid for NdNiO_3 . We recall that in the case of $R\text{NiO}_3$ systems ($R = \text{Nd, Pr, Sm, ...}$), the gap E_g is approximated by $E_g = \Delta - W$, where Δ and W are the charge transfer and the O_{2p} -like band width, respectively.^{26,27,33} Since NdNiO_3 is a distorted perovskite, W is given as $W \approx W_0 \cos(w)$, where $W_0 \sim 1$ eV and w are the bandwidth of nondistorted perovskite and the tilt angle, respectively, with $\theta = 180^\circ - 2w$ as the angle of the bond Ni-O-Ni. Since Δ does not change so much as a function of temperature,^{26,27} we obtain $\frac{\partial E_g}{\partial P} \approx \frac{\partial w}{\partial P} W_0 \sin(w)$. At 5 K, $\frac{\partial w}{\partial P} \sim 1.5 \times 10^{-10}$ rad Pa⁻¹ (Ref. 26) for PrNiO_3 compound, which leads to $\frac{\partial E_g}{\partial P} \approx -0.5 \times 10^{-12}$ eV Pa⁻¹.

From our studies, one can get an estimate of that deformation-potential parameter. As a rough approximation, we can consider that the electronic stress reduces to $\sum_{\vec{k}} \Delta n_e(\vec{k}) \frac{\partial E_{\vec{k}}}{\partial \eta_{ij}} = -NB \frac{\partial E_g}{\partial P}$,^{2,7,8} with $E_g \approx \Delta - W$ as the pseudogap. Then if we consider the equality between the thermoelastic ($\sigma_p = -3B\beta\Delta T_L$) and the electronic stresses, this leads to the estimate $\frac{\partial E_g}{\partial P} \sim -7 \times 10^{-11}$ eV Pa⁻¹ with a thermal-expansion coefficient β of $\sim 10^{-5}$ K⁻¹, a bulk elastic modulus of B

$\sim 10^{11}$ Pa, and a pump-induced lattice temperature increase of $\Delta T_L \sim 20$ K (typical photoexcitation of 10^{19} cm $^{-3}$). This analysis shows that our estimate is more than ten times larger than that obtained from the analysis of the pressure dependence of the electronic properties of NdNiO $_3$. It is interesting to note that such a deformation-potential parameter is close in magnitude to that found for the polar semiconductor GaAs ($\frac{\partial E_g}{\partial P} \sim +10 \times 10^{-11}$ eV Pa $^{-1}$, for the Brillouin-zone center Γ valley),⁶ which is a well-known compound where the electronic stress is larger than the thermoelastic one. To describe more precisely the microscopic origin of the electronic contribution in the case of NdNiO $_3$, i.e., to attribute the electronic stress to a contribution of a particular electronic level (polaronic level), it will be necessary to characterize the optical properties under pressure at least. Such data do not exist yet to the best of our knowledge.

(ii) The second important result we want to discuss is the absence of a change in acoustic pulse sign in the region $T \sim T_{MI}$ as would be expected if the generation process is driven by thermoelasticity. This result suggests either that a nonthermal process dominates or that the thermoelastic process, if dominant, is driven by a thermal-expansion coefficient which at short time scales is different from that measured at thermodynamic equilibrium conditions (that deduced from x-ray-diffraction studies). The nonthermal process contribution can be considered here but according to literature²³ and, if correct, to our previous discussion presented in part (i), the deformation-potential stress would still be positive ($\frac{\partial E_g}{\partial \eta} > 0$) in the temperature range of the coexisting insulating and metallic phases, and thus cannot compete with thermoelasticity, which has become positive since the thermal coefficient has turned to negative values (see Fig. 1). On the contrary both contributions should add. In reality we do not have evidence of such an effect. More likely, there is another possible explanation which deserves to be discussed and which could explain the experimental results in that temperature range ($T \sim T_{MI}$). The MIT is described as a first-order phase transition. Consequently in the critical temperature range we discuss here, there is a coexistence of two phases, namely, the metallic and the insulating phases. This coexistence has also been evidenced by electrical conductivity measurements.^{43,44} Therefore, the measured lattice parameter in that temperature range is a mixture of lattice parameters of the low- and high-temperature phases weighted by the concentration of these phases. The mean lattice parameter is

$$a(T) = \alpha_m(T)a_m(T) + [1 - \alpha_m(T)]a_i(T), \quad (4)$$

where $\alpha_m(T)$ is the fraction of the unit volume occupied by the metallic phase (m) at a given temperature T . a_m and a_i are the lattice parameters of the metallic and insulating phases, respectively. For $T \ll T_c$, $\alpha_m(T) = 0$ and $T \gg T_c$, $\alpha_m(T) = 1$. T_c is a critical temperature where both phases exist.

Since the metallic phase has a smaller lattice parameter than that of the insulating phase [see Fig. 1(b)] for $T \sim T_{MI}$, when the temperature slightly increases, the apparent lattice parameter decreases following the decrease in the volumic fraction of the insulating state. This kinetic process is a

rather slow process controlled by an atomic diffusion process and heat transfer between the two metastable phases. We have estimated the characteristic length l_H corresponding to the heat diffusion over the typical time scale of the acoustic pulse duration $\tau_a \sim 20$ ps. For that estimation, we have determined the heat diffusion coefficient D from the values of the heat conductivity $\kappa = 5$ W m $^{-1}$ K $^{-1}$,⁴⁵ and the heat capacity $C_L(180$ K) = 3×10^6 J m $^{-3}$ K $^{-1}$,²⁰ according to $D = \kappa / C_L$. We have found $l_H \sim 6$ nm, which is much smaller than any dimension of the pump-irradiated volume where both photo-generation and photodetection take place. As a consequence, it is important to underline that when a femtosecond laser-pulse excites the system, the energy provided by the laser and absorbed by the system cannot produce a rapid change in the concentration of both phases (latent heat) which consequently leads to $\frac{d\alpha_m(T)}{dT} \approx 0$. More likely, during that first step taking place on a picosecond time scale, only the number of phonons are locally and rapidly increased in each metastable insulating or metallic phase. We can consider finally that the laser excites the insulating and metallic phases at the same time but there is no growth of the metallic domains. Since both phases have their own positive thermal-expansion coefficients (β_m and β_i), the magnitude of the laser-induced acoustic pulse can then be described by a summation of two thermoelastic contributions arising from the metallic and insulating phases. During the time of generation of coherent acoustic phonons, the mean thermal-expansion coefficient is given by

$$\beta(T) = \frac{da(T)}{dT} \approx \alpha_m(T)\beta_m(T) + [1 - \alpha_m(T)]\beta_i(T). \quad (5)$$

This thermal-expansion coefficient is then always positive, in agreement with the experimental observations.

III. SUMMARY

In this work, time-resolved optical measurements were performed on the metal-insulator transition compound NdNiO $_3$. The acoustical phonon photogeneration processes were studied. It appears that in addition to thermal stress arising from rapid heating of the lattice, some nonclassical processes are involved. On one hand, for $T < T_{MI}$, we can attribute it qualitatively at least partially to the manifestation of the deformation-potential mechanism (compressive photo-induced stress) and we connect it to the ability of the lattice to contract under photodoping. The corresponding microscopic effect of that deformation-potential process would be an ultrafast laser-induced reduction in charge disproportionation on the Ni sites which then yields to lattice cell volume decrease (compressive stress). On the other hand, in the critical temperature range $T \approx T_{MI}$, where both insulating and metallic phases exist, the temperature dependence of the acoustic pulse magnitude exhibits clear departure from that predicted by the pure thermoelastic model. The understanding of this phenomenon is not definitive yet. Nevertheless, we suggest that the thermodynamic thermal-expansion coefficient determined by x-ray-diffraction studies may not be the relevant parameter for estimating the laser-induced thermoelastic stress contribution in the metastable state. The

negative value of the thermal-expansion coefficient deduced from x-ray-diffraction studies is due to the change in the volumic fraction of each of the insulating and metallic phases when the temperature is varied. However, since such phase transformation from insulating (metallic) metastable phase to metallic (insulating) one is a slow process, at the very short time scale of phonon photogeneration the volumic fraction of each of the two phases cannot change. Consequently, additive contribution of the metallic and insulating metastable phases to the thermoelastic stress (without modi-

fication of the relative magnitude of these separated contributions) is more likely to occur. Our approach explains the experimental observations at least qualitatively. In perspective, since atomic displacements can be directly measured by x-ray diffraction, time-resolved x-ray diffraction^{14,15,46} could provide further information on the ability of the lattice to contract or expand when submitted to ultrafast optical excitation. Atomic displacements can also be determined with the optical pump-probe method but using deflectometry setup.⁷ These possibilities will be studied in the near future.

*pascal.ruello@univ-lemans.fr

- ¹C. Thomsen, J. Strait, Z. Vardeny, H. J. Maris, J. Tauc, and J. J. Hauser, *Phys. Rev. Lett.* **53**, 989 (1984).
- ²C. Thomsen, H. T. Grahn, H. J. Maris, and J. Tauc, *Phys. Rev. B* **34**, 4129 (1986).
- ³V. Gusev and A. Karabutov, *Laser Optoacoustics* (AIP, New York, 1993).
- ⁴R. Merlin, *Solid State Commun.* **102**, 207 (1997).
- ⁵Y.-X. Yan, E. B. Gamble, Jr., and K. A. Nelson, *J. Chem. Phys.* **83**, 5391 (1985).
- ⁶N. E. Christensen and I. Gorczyca, *Phys. Rev. B* **50**, 4397 (1994).
- ⁷O. B. Wright and V. E. Gusev, *Appl. Phys. Lett.* **66**, 1190 (1995).
- ⁸O. B. Wright, B. Perrin, O. Matsuda, and V. E. Gusev, *Phys. Rev. B* **64**, 081202(R) (2001).
- ⁹R. W. Schoenlein, W. Z. Lin, J. G. Fujimoto, and G. L. Eesley, *Phys. Rev. Lett.* **58**, 1680 (1987).
- ¹⁰V. E. Gusev and O. B. Wright, *Phys. Rev. B* **57**, 2878 (1998).
- ¹¹Fausto Rossi and Tilmann Kuhn, *Rev. Mod. Phys.* **74**, 895 (2002).
- ¹²Neil W. Ashcroft and N. David Mermin, *Solid State Physics* (Saunders, Philadelphia, 1976).
- ¹³D. Lim, V. K. Thorsmølle, R. D. Averitt, Q. X. Jia, K. H. Ahn, M. J. Graf, S. A. Trugman, and A. J. Taylor, *Phys. Rev. B* **71**, 134403 (2005).
- ¹⁴C. v. Korff Schmising, A. Harpoeth, N. Zhavoronkov, Z. Ansari, C. Aku-Leh, M. Woerner, T. Elsaesser, M. Bargheer, M. Schmidbauer, I. Vrejoiu, D. Hesse, and M. Alexe, *Phys. Rev. B* **78**, 060404(R) (2008).
- ¹⁵C. v. Korff Schmising, M. Bargheer, M. Kiel, N. Zhavoronkov, M. Woerner, T. Elsaesser, I. Vrejoiu, D. Hesse, and M. Alexe, *Phys. Rev. Lett.* **98**, 257601 (2007).
- ¹⁶J. E. Lorenzo, J. L. Hodeau, L. Paolasini, S. Lefloch, J. A. Alonso, and G. Demazeau, *Phys. Rev. B* **71**, 045128 (2005).
- ¹⁷J. L. Garcia-Munoz, J. Rodriguez-Caracals, P. Lacorre, and J. B. Torrance, *Phys. Rev. B* **46**, 4414 (1992).
- ¹⁸X. Granados, J. Fontcuberta, X. Obradors, Ll. Manosa, and J. B. Torrance, *Phys. Rev. B* **48**, 11666 (1993).
- ¹⁹M. Medarde, *J. Phys.: Condens. Matter* **9**, 1679 (1997).
- ²⁰J. Blasco, M. Castro, and J. Garcia, *J. Phys.: Condens. Matter* **6**, 5875 (1994).
- ²¹F. Capon, P. Ruello, J.-F. Bardeau, P. Simon, P. Laffez, B. Dkhil, L. Reversat, K. Galicka, and A. Ratuszna, *J. Phys.: Condens. Matter* **17**, 1137 (2005).
- ²²T. Katsufuji, Y. Okimoto, T. Arima, Y. Tokura, and J. B. Torrance, *Phys. Rev. B* **51**, 4830 (1995).
- ²³M. Medarde, D. Purdie, M. Grioni, M. Hengsberger, Y. Baer, and P. Lacorre, *Europhys. Lett.* **48**, 11666 (1993).
- ²⁴I. Vobornik, L. Perfetti, M. Zacchigna, M. Grioni, G. Margaritondo, J. Mesot, M. Medarde, and P. Lacorre, *Phys. Rev. B* **60**, R8426 (1999).
- ²⁵K. Okazaki, T. Mizokawa, A. Fujimori, E. V. Sampathkumaran, M. J. Martinez-Lope, and J. A. Alonso, *Phys. Rev. B* **67**, 073101 (2003).
- ²⁶M. Medarde, J. Mesot, P. Lacorre, S. Rosenkranz, P. Fischer, and K. Gobrecht, *Phys. Rev. B* **52**, 9248 (1995).
- ²⁷X. Obradors, L. M. Paulius, M. B. Maple, J. B. Torrance, A. I. Nazzal, J. Fontcuberta, and X. Granados, *Phys. Rev. B* **47**, 12353 (1993).
- ²⁸P. C. Canfield, J. D. Thompson, S.-W. Cheong, and L. W. Rupp, *Phys. Rev. B* **47**, 12357 (1993).
- ²⁹P. Ruello, B. Perrin, T. Pezeril, V. E. Gusev, S. Gougeon, N. Chigarev, P. Laffez, P. Picart, D. Mounier, and J.-M. Breteau, *Physica B* **363**, 43 (2005).
- ³⁰B. Perrin, C. Rossignol, B. Bonello, and J.-C. Jeannet, *Physica B* **263-264**, 571 (1999).
- ³¹P. Laffez, R. Retoux, P. Boullay, M. Zaghrioui, P. Lacorre, and G. Ventendeloo, *Eur. Phys. J.: Appl. Phys.* **12**, 55 (2000).
- ³²P. Ruello, S. Zhang, P. Laffez, B. Perrin, and V. Gusev, *Phys. Rev. B* **76**, 165107 (2007).
- ³³J. B. Torrance, P. Lacorre, A. I. Nazzal, E. J. Ansaldo, and C. H. Niedermayer, *Phys. Rev. B* **45**, 8209 (1992).
- ³⁴J.-Y. Duquesne and B. Perrin, *Phys. Rev. B* **68**, 134205 (2003).
- ³⁵D. H. Hurley and O. B. Wright, *Opt. Lett.* **24**, 1305 (1999).
- ³⁶For the simulation of the transient optical signal (ρ and $\delta\phi$), the surface displacement and propagating acoustic strain were $\delta z(z=0, t) = -\frac{\eta_0 f_{ac}}{\alpha} e^{-\alpha v|t|}$ and $\eta(z, t) = \frac{\eta_0 f_{ac}}{2} [e^{\alpha|z-vt|} \text{sgn}(z-vt) + e^{\alpha|z+vt|} \text{sgn}(z+vt)]$. η_0 , v , and α are the magnitude of the photoinduced acoustic strain, the sound speed, and the optical-absorption coefficient.
- ³⁷T. Mizokawa, A. Fujimori, T. Arima, Y. Tokura, N. Mori, and J. Akimitsu, *Phys. Rev. B* **52**, 13865 (1995).
- ³⁸M. Zaghrioui, A. Bulou, P. Lacorre, and P. Laffez, *Phys. Rev. B* **64**, 081102(R) (2001).
- ³⁹U. Staub, G. I. Meijer, F. Fauth, R. Allenspach, J. G. Bednorz, J. Karpinski, S. M. Kazakov, L. Paolasini, and F. d'Acapito, *Phys. Rev. Lett.* **88**, 126402 (2002).
- ⁴⁰M. Medarde, P. Lacorre, K. Conder, F. Fauth, and A. Furrer, *Phys. Rev. Lett.* **80**, 2397 (1998).

- ⁴¹N. E. Massa, J. A. Alonso, M. J. Martinez-Lope, and I. Rasines, *Phys. Rev. B* **56**, 986 (1997).
- ⁴²J. Rodriguez-Carvajal, S. Rosenkranz, M. Medarde, P. Lacorre, M. T. Fernandez-Diaz, F. Fauth, and V. Trounov, *Phys. Rev. B* **57**, 456 (1998).
- ⁴³G. Catalan, R. M. Bowman, and J. M. Gregg, *Phys. Rev. B* **62**, 7892 (2000).
- ⁴⁴G. Catalan, *Phase Transitions* **81**, 729 (2008).
- ⁴⁵J. S. Zhou, J. B. Goodenough, and B. Dabrowski, *Phys. Rev. B* **67**, 020404(R) (2003).
- ⁴⁶F. S. Krasniqi, S. L. Johnson, P. Beaud, M. Kaiser, D. Grolimund, and G. Ingold, *Phys. Rev. B* **78**, 174302 (2008).